**RAPID COMMUNICATION**

# Atomic optical spatial mode extractor for vector beams based on polarization-dependent absorption

Hong Chang(常虹)[1,2], Xin Yang(杨欣)[3], Jinwen Wang(王金文)[3], Yan Ma(马燕)[1,2], Xinqi Yang(杨鑫琪)[1,2], Mingtao Cao(曹明涛)[1,2,†], Xiaofei Zhang(张晓斐)[1,2], Hong Gao(高宏)[3], Ruifang Dong(董瑞芳)[1,2,‡], and Shougang Zhang(张首刚)[1,2,§]

[1] *Key Laboratory of Time and Frequency Primary Standards, National Time Service Center, Chinese Academy of Sciences, Xi'an* 710600, *China*
[2] *School of Astronomy and Space Science, University of Chinese Academy of Sciences, Beijing* 100049, *China*
[3] *Ministry of Education Key Laboratory for Nonequilibrium Synthesis and Modulation of Condensed Matter, Shaanxi Province Key Laboratory of Quantum Information and Quantum Optoelectronic Devices, School of Physics, Xi'an Jiaotong University, Xi'an* 710049, *China*

(Received 2 November 2022; revised manuscript received 6 December 2022; accepted manuscript online 16 December 2022)

Vector beams with spiral phase and spatially varying polarization profiles have many applications from optical micromanipulation to materials processing. Here, we propose and demonstrate an atomic spatial mode extracting scheme for the vector beam based on polarization-dependent absorption in the atom vapor. By employing the linear polarization pump beam which induces polarization sensitive absorption in the atomic ensemble, a counter-propagated weak probe vector beam is extracted by spatial absorption, and extracted part still maintains the original polarization and the vortex phase. The topological charges of the extracted mode are verified by interfering with the Gaussian beam, and it can be found that the orbital angular momentum is conserved in the extracting process. Our work will have potential applications in non-destructive spatial mode identification, and is also useful for studying higher-dimensional quantum information based on atomic ensembles.

**Keywords:** vector beam, polarization-dependent absorption, optical pumping

**PACS:** 42.50.–p, 42.25.Ja, 32.80.Qk, 82.53.Kp **DOI:** 10.1088/1674-1056/acac19

## 1. Introduction

Vector beams (VBs) with spatially nonuniform polarization and phase distribution have attracted much interest for their potential applications in optical manipulation,[1,2] optical trapping,[3,4] and quantum communication.[5–7] The VBs, maintaining two orthogonal circular polarizations with opposite orbital angular momentum (OAM), are usually selected as the good candidate for coding hybrid quantum states in quantum information protocols.[8,9] Essentially, the VBs carry a form of entanglement in their two degrees of freedom, which can represent classically entangled light, and are widely used in quantum communication.[10–12]

Within this context, the capability of coherently interacting VBs with atoms could open a variety of applications.[13–20] The coherent manipulation of this kind of structured light will enable the extension of these promises to applications such as quantum information involving high-dimensional entanglement state coding. Besides quantum information, the combination of the peculiar properties of structured light with atoms can lead to novel applications, such as ultrasensitive magnetometers.[21,22] Recently, several attempts were engaged to extract the "authentic basis" of VBs with arbitrary polarization distribution in an atomic vapor,[23,24] and these direct projective measurements based on the atom–light interface provide new tools for atomic physics and polarization optics.[25]

In this paper, we propose a scheme for extracting the basis modes of VBs based on polarization-dependent absorption in atom vapor. Principally, the OAM and Hermite–Gaussian (HG) modes can be directly extracted from the VBs based on the optical pumping effect. We find that the patterns of transmission and interference are changing with the alteration in polarized states of the pump light field, and the fringes of the two cases all show high contrast. In the meantime, we analyze the behavior of the probe beam by inspecting the polarization-dependent absorption, and the results are in good consistence with the theoretical analyses.

## 2. Experimental setup

Figure 1 illustrates the experimental setup. The laser beam from the DL 100 (795 nm) is divided into two parts by a polarizing beam splitter (PBS). One part is used for frequency locking to the $5S_{1/2}, F = 2 \rightarrow 5P_{1/2}, F' = 1$ transition of $^{87}$Rb D1 line, as shown in Fig. 1(a). The other one is collected by a single-mode optical fiber (SMF) to optimize the spatial mode. Afterward, the beam passes through the combination

†Corresponding author. E-mail: mingtaocao@ntsc.ac.cn
‡Corresponding author. E-mail: dongruifang@ntsc.ac.cn
§Corresponding author. E-mail: szhang@ntsc.ac.cn

© 2023 Chinese Physical Society and IOP Publishing Ltd 

of a half-wave plate (HWP1) and PBS1, and the intensities of reflected and transmitted outputs from PBS1 are fixed at 2 mW and 40 μW, respectively. As depicted in Fig. 1(b), the transmitted beam from PBS1 is then converted to the second-order vector beam (VB) by using a Q-plate with $m = 2$, and used as the probe beam. The reflected beam is further divided into two parts by utilizing PBS2. The reflected part is selected as the reference beam to analyze the experimental results, and the other one is used as the pump beam. By adjusting the combination of HWP2 and a QWP, the polarization state of the pump beam will be changed from linear to circular. After passing through a beam splitter (BS), the pump beam is injected into a 5-cm-long rubidium cell, and precisely counter-propagates with the probe beam. A three-layer μ-metal magnetic shield is used to isolate the cell from ambient magnetic fields. The temperature of the cell is set at 65 °C with a controller. In our experiment, the quantization axis is defined along the direction of the pump beam propagation. As shown in Fig. 1(c), after passing through the cell, the probe beam is injected into the Mach–Zehnder interferometer and interferes with the reference beam. The spatial intensity distribution of interference is recorded by a charge-coupled device camera (CCD).

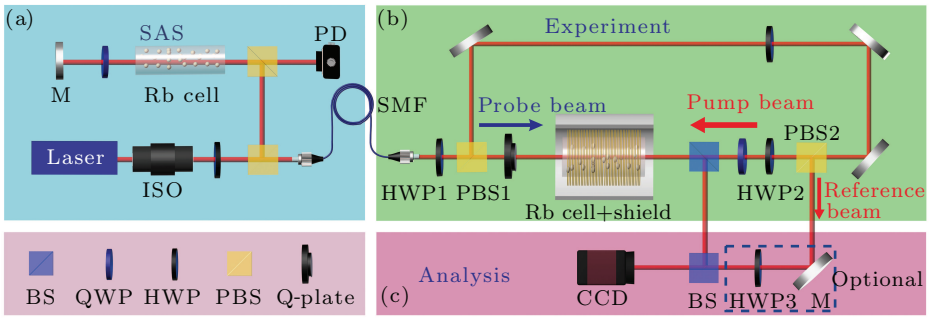



**Fig. 1.** Experimental setup: (a) the local system, (b) the manipulation of the vector beam, (c) the mode analysis of the probe beam. PBS: polarizing beam splitter, HWP: half-wave plate, QWP: quarter-wave plate, ISO: optical isolator, M: mirror, PD: photodetector, SMF: single-mode optical fiber, BS: beam splitter, CCD: charge-coupled device camera. The inner yellow coil between the two shields is the heating coil.

## 3. Results and discussion

In Fig. 2(a), we construct the setup to obtain the Stokes parameters of the probe beam by the projection measurement method. By putting it directly after the Q-plate in Fig. 1(b), the polarization distribution of the second-order VB is observed by measuring the Stokes parameters. All linear polarization components can be determined by rotating the HWP, and the left- or right-handed circularly polarized components can be selected by superimposing the QWP. Figure 2(b) shows the results for different Stokes parameters, in which $S_1$ represents the vertical and horizontal, $S_2$ stands for 45° and 135°, and $S_3$ describes the left- and right-handed circularly polarized components of VB. Figure 2(c) indicates both the polarization and spatial intensity distribution of VB, which are reconstructed by coding with a program in MATLAB. According to Figs. 2(b) and 2(c), the probe beam only includes linear polarization.

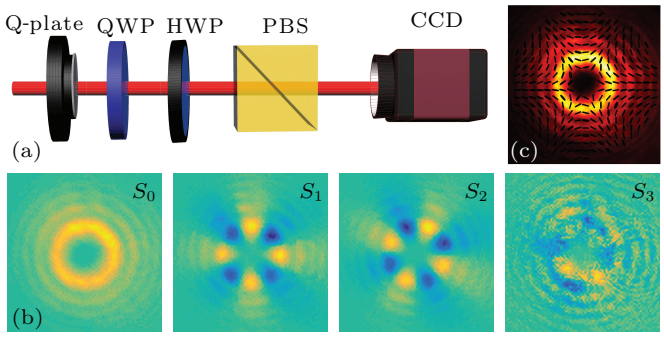



**Fig. 2.** (a) Experimental setup of Stokes parameters measurement. (b) Stokes parameters of vector beam. (c) Reconstructed polarization distribution of vector beam. The black lines indicate linear polarization.

### 3.1. The extraction of HG modes of VBs

Now we turn our attention to the experiment shown in Fig. 1(b). First, the QWP is taken away and the optical axis of the HWP2 is set along the horizontal direction. Here, the polarization state of the pump beam is horizontal when the rotation angle $\theta$ is set to 0°. After passing through the rubidium cell, a four-petal pattern of transmitted intensity distribution pattern is recorded on the CCD for the original probe beam, which is shown in Fig. 3(a). The polarization component of the probe beam in the vertical and horizontal direction is absorbed while that in the diagonal direction is transmitted. Therefore, the transmission mode of the probe beam is exactly consistent with $HG_{11}$.

In Fig. 3(a), the intensity distribution of the probe beam changes from its original donut-shaped pattern to a four-petal pattern. We also observed that the four-petal pattern rotates with the fast axis of the HWP2, while the rotation angle is exactly synchronized with the HWP2. The experimental results show that the specific polarization of the pump beam can determine the transmission of the probe beam in a specific position.

Figure 3(b) depicts the normalized transmission intensity of the probe beam with $\varphi$ from 0° to 180°. The range of $\varphi$ is chosen from 0° to 180° in Fig. 3(b), which is exactly one period, and this can present a full picture of the transmission intensity. As depicted in the first figure of Fig. 3(a), the range of angle $\varphi$ is shown as the numbers and lines. Here, we get the same dotted circle (the center of intensity distribution patterns

is the center of the circle) from the corresponding patterns with various angles, and analyze the changes in their normalized intensity. As shown in Fig. 3(b), with the $\varphi$ increased, the peak intensities appear in the same counting interval and the transmittance contrast of the probe beam is close to 1.

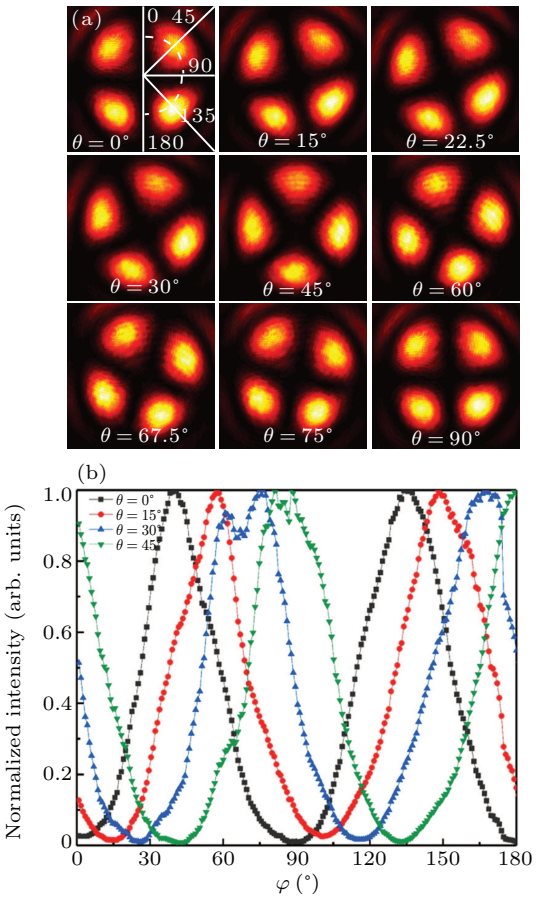



**Fig. 3.** The experimental results for (a) the manipulation of vector beam (by only using an HWP) with various $\theta$ and (b) the probe transmission plotted as a function of different angles ($\varphi$).

### 3.2. The extraction of OAM modes of VBs

The VB can be expressed by different basis vectors. By putting QWP back into the setup, the extraction of the OAM mode of the probe beam can also be realized. Keeping the angle of QWP at 0° and rotating the HWP2 in the pump light field from 0° to 90°, we observed the four-petal patterns rotate with various $\theta$. However, the transmission intensity distribution of the probe beam is changed to a donut-shaped intensity profile when the $\theta$ is set to 22.5°, which means the polarization state of the pump beam is circular polarized.

Here, the intensity distribution pattern at $\theta = 90°$ is consistent with that at $\theta = 0°$. With the left-handed circularly polarized pump beam at $\theta = 22.5°$, as shown in Fig. 4(a), almost all of the probe beam is transmitted so that its intensity distribution shows like a "donut". And the transmission mode of the light field is exactly consistent with the OAM mode with the topological charge $l = 2$. Similarly, when the angle is rotated to 67.5°, the pump beam is right-handed circularly polarized, and the intensity distribution is also like a "donut".

As a result, the extracted four-petal pattern rotates by varying the polarization of the pump beam. Experimentally, the donut-shaped intensity profile can be obtained by using a QWP.

Figure 4(b) gives the intensity profile of the extracted OAM pattern from VBs. It is obvious that the image contrast is getting worse when changing the polarization of the pump beam to circular polarization by rotating the phase angle $\theta$, which displays the intensity distribution of OAM modes. It is reasonable that the results are different with the case of extracting HG modes shown in Fig. 3(b), since the OAM modes are extracted from VBs with the circular pump beam in this condition.

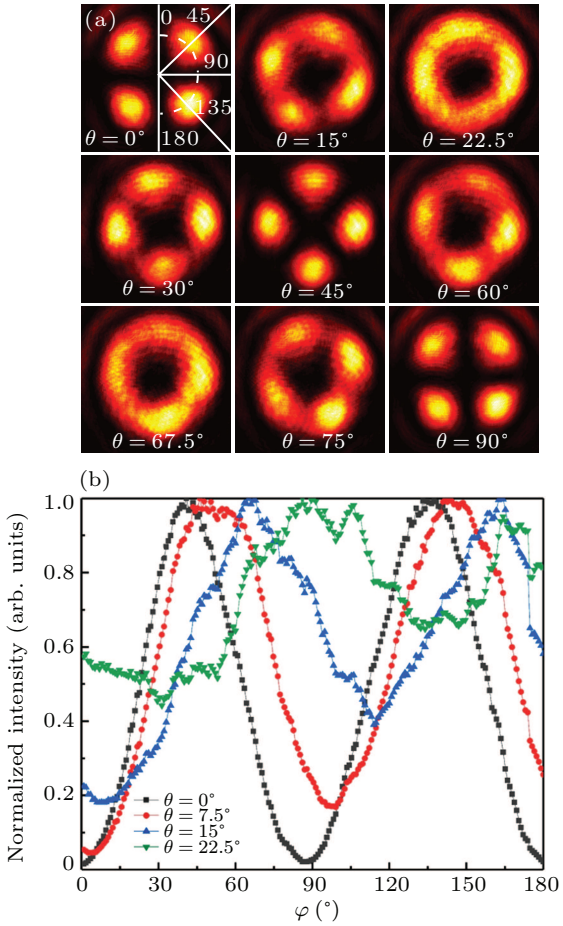



**Fig. 4.** The experimental results for (a) the manipulation of vector beam (by using an HWP and a QWP) with various $\theta$ and (b) the transmission of the probe beam plotted as a function of different angles ($\varphi$).

### 3.3. The phase reconfiguration of basis modes of vector beam

Interference can effectively verify the extracted phase information of the basis modes of the vector probe beam, as shown in Fig. 1(c). The reflected beam from PBS2 is selected as a reference beam whose polarization can be adjusted by HWP3, and then interference with the probe beam at BS before the CCD. Finally, the interference pattern is recorded by a charge-coupled device camera. And the results as shown in Fig. 5.

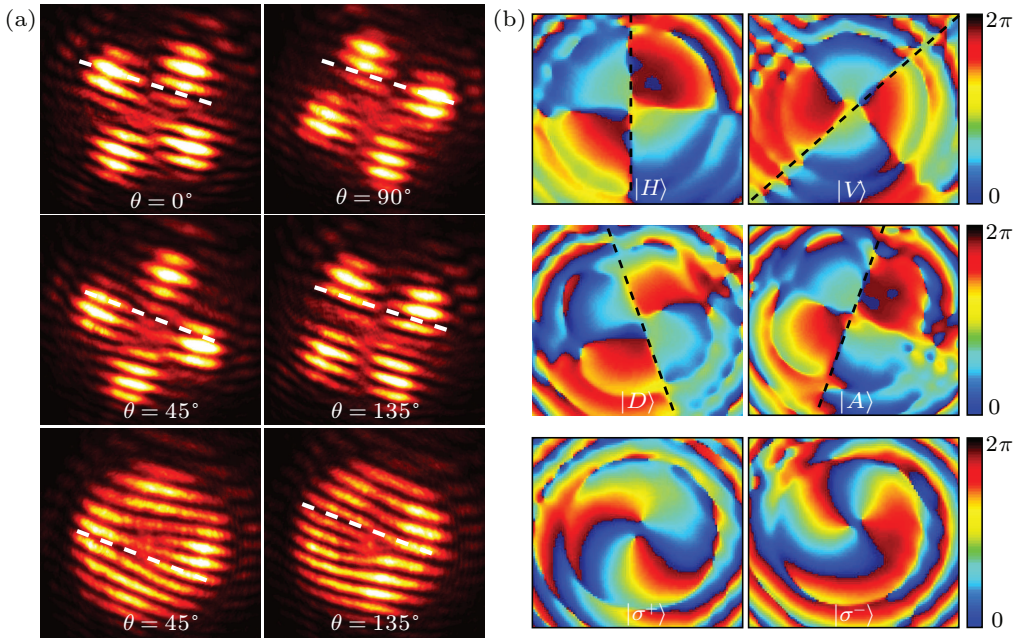



**Fig. 5.** (a) The interference intensity distribution and (b) the phase reconfiguration of basis modes of vector beam.

As figure 5(a) shows, the intensity distribution has exhibited the interference results between the reference beam and the six basic modes of the vector probe beam. The first two rows indicate the extracted basic modes of the probe beam when the polarized state of the pump beam is horizontally polarized state, vertically polarized state, and linear $+45^\circ$ and linear $-45^\circ$ polarized state, respectively. The third row shows the extracted basic modes when the pump beam is left- and right-handed circularly polarized states. At the same level of the white reference line in the first figure of Fig. 5(a), the brightness of each peak is changed, which clearly reflects the $\pi$ phase difference between each peak. In contrast, the third row shows a forked interference structure. To present the phase information of extracted basis modes from the vector probe beam, we reconstruct the phase image shown in Fig. 5(b). It is observed that the first two rows of Fig. 5(b) are the phase distribution corresponding to the pattern at the same position as Fig. 5(a), which depicts the phase distribution of HG modes respectively. However, the phase distribution with vortex characteristics is shown in the third row of Fig. 5(b). So far, we have already successfully verified the phase distribution of the basic mode extracted from the vector probe beam by using the polarization-dependent absorption effect based on hot atomic ensembles.

In order to understand the coupling between atoms and the pump and probe beams carrying different polarized states when these two beams are counter-propagating with each other, we analyze the coupling effect in the Zeeman sub-levels of $^{87}$Rb as shown in Fig. 6. The pump and probe beams with the same or orthogonal linear polarization are shown in Figs. 6(a) and 6(b), respectively. The pump beam with the right-handed circularly polarized state is shown in Fig. 6(c) and the left-handed circularly polarized state is shown in Fig. 6(d).

In Figs. 6(a) and 6(b), there are two types of coupling beams of the linearly polarized state. As figure 6(a) shows, when the polarization direction of the pump beam agrees with that of the probe, the pump beam couples $5S_{1/2}F = 2$, $m_F = -1,\ 0,\ +1$ to $5P_{1/2}F' = 1$, $m_F = -1,\ 0,\ +1$ transition. And most atoms will be pumped to the ground state of $5S_{1/2}F = 2, m_F = -2, +2$, which induced the maximum transmission of the probe beam. As shown in Fig. 6(b), when the polarization direction of the pump beam is orthogonal to the probe beam, most atoms will be pumped in the ground state in $5S_{1/2}F = 2$, $m_F = -2, +2$. But due to the quantization of the pump beam, the probe beam is decomposed into the left- and right-handed circularly polarized beams to interact with atoms. Thus, the absorption of the probe beam is increased. That is why the four-petal intensity distribution appears by using the linear polarized state of the pump beam.

As shown in Fig. 6(c), the pump beam with the left-handed circularly polarized state couples $5S_{1/2}F = 2$, $m_F = -2,\ -1,\ 0$ to $5P_{1/2}F' = 1$, $m_F = -1,\ 0,\ +1$ transitions and pumps most atoms to the energy state of $5S_{1/2}F = 2$, $m_F = +1,\ +2$. Here, the probe beam is also divided into left- and right-handed circularly polarized beams coupled with atoms. The left-handed circularly polarized components are transmitted and the right-handed circularly polarized components are absorbed. A similar explanation can verify the situation in Fig. 6(d).

Hence, the specific polarization and mode extraction of vector beams can be realized effectively by adjusting the polarization of the pump beam through the polarization-dependent absorption effect.

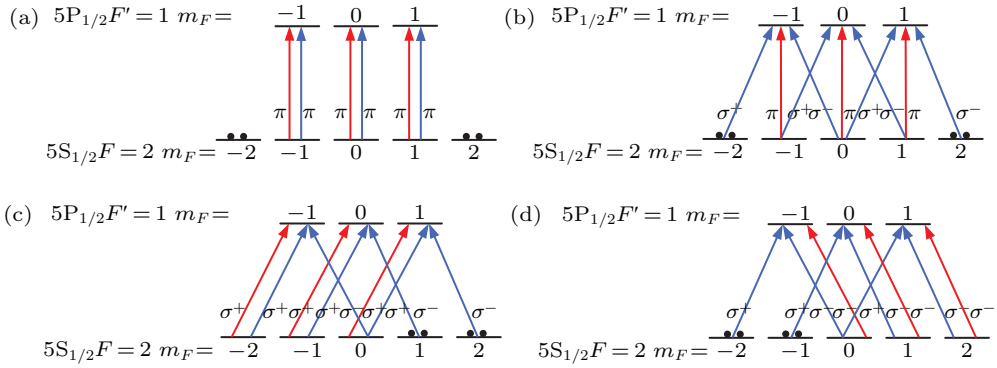



**Fig. 6.** Schematic diagrams of the (a) linearly, (b) linearly, (c) left-handed circularly, and (d) right-handed circularly polarized pump and the linearly polarized probe beams in different polarized coupling processes with atoms. The red line represents the coupling of the pump beam, and the blue line represents the coupling of the probe beam.

## 4. Conclusion

In conclusion, we reported an atomic spatial mode extracting scheme of vector beams based on polarization-dependent absorption in the hot atom ensembles. By employing the different polarization states of the pump beam, we find that the HG mode can be extracted by using a linearly polarized pump beam, and the OAM mode can be extracted when the polarization of the pump beam become a left- or right-handed circularly polarized state. The interaction analyses between light and atoms at specific energy levels can explain our results perfectly. Furthermore, our research can be used for non-destructive spatial mode identification of atom ensemble in the quantum memory system. Compared to linear optical polarization, our experimental scheme may provide a convenient and higher-dimensional polarization selection method for VB manipulation based on atomic ensembles. In addition, it also will play an important role in quantum computation and information transmission.

## References


[1] Epstein M S, Bayer S, Bradshaw J, Voigtman E and Winefordner J D 1980 *Spectrochim Acta Part B At. Spectrosc.* **35** 233
[2] Li S M, Ren Z C, Kong L J, Qian S X, Tu C H, Li Y N and Wang H T 2016 *Photon. Res.* **4** B29
[3] Wang X L, Chen J, Li Y N, Ding J P, Guo C S and Wang H T 2010 *Phys. Rev. Lett.* **105** 253602
[4] Gao X Z, Pan Y, Zhang G L, Zhao M D, Ren Z C, Tu C G, Li Y N and Wang H T 2017 *Photon. Res.* **5** 640
[5] Barreiro J T, Wei T C and Kwiat P G 2010 *Phys. Rev. Lett.* **105** 030407
[6] Fickler R, Lapkiewicz R, Ramelow S and Zeilinger A 2014 *Phys. Rev. A* **89** 060301
[7] Milione G, Nguyen T A, Leach J, Nolan D A and Alfano R R 2015 *Opt. Lett.* **40** 4887
[8] Milione G, Sztul H I, Nolan D A and Alfano R R 2011 *Phys. Rev. Lett.* **107** 053601
[9] Guzmán C R, Ndagano B and Forbes A 2018 *J. Opt.* **20** 123001
[10] D'Ambrosio V, Nagali E, Walborn S P, Aolita L, Slussarenko S, Marrucci L and Sciarrino F 2012 *Nat. Commun.* **3** 961
[11] Karimi E and Boyd R W 2015 *Science* **350** 1172
[12] Sit A, Bouchard F, Fickler R, Gagnon-Bischoff J, Larocque H, Heshami K, Elser D, Peuntinger C, Günthner K, Heim B, Marquardt C, Leuchs G, Boyd R W and Karimi E 2017 *Optica* **4** 1006
[13] Youngworth K S and Brown T G 2000 *Opt. Express* **7** 77
[14] Zhan Q W 2009 *Adv. Opt. Photon.* **1** 1
[15] Milione G, Lavery M P, Huang H, Ren Y X, Xie G D, Nguyen T A, Karimi E, Marrucci L, Nolan D A, Alfano R R and Willner A E 2015 *Opt. Lett.* **40** 1980
[16] Drevinskas R, Zhang J Y, Beresna M, Gecevičius M, Kazanskii A G, Svirko Y P and Kazansky P G 2016 *Appl. Phys. Lett.* **108** 221107
[17] Xu H F, Zhang R, Sheng Z Q and Qu J 2019 *Opt. Express* **27** 23959
[18] Wang C F, Yang B, Cheng M L, Cheng S H, Liu J M, Xiao J N, Ye H P, Li Y, Fan D Y and Chen S Q 2020 *Opt. Express* **28** 38666
[19] Zhang Y Q, Hou T Y, Chang H X, Yu T, Chang Q, Jiang M, Ma P F, Su R T and Zhou P 2021 *Opt. Express* **29** 5259
[20] Dong Z P, Zhang Y M, Li H X, Dong Z P, Zhang Y M, Li H X, Tao R X, Gu C, Yao P J, Zhan Q W and Xu L X 2021 *Opt. Laser Technol.* **139** 106965
[21] Castellucci F, Clark T W, Selyem A, Wang J W and Franke-Arnold S 2021 *Phys. Rev. Lett.* **127** 233202
[22] Qiu S W, Wang J W, Castellucci F, Cao M T, Zhang S G, Clark T W, Franke-Arnold S, Gao H and Li F L 2021 *Photon. Res.* **9** 2325
[23] Wang J W, Yang X, Dou Z H, Qiu S W, Liu J, Chen Y, Cao M T, Chen H X, Wei D, Müller-Dethlefs K, Gao H and Li F L 2019 *Appl. Phys. Lett.* **115** 221101
[24] Wang J W, Chen Y, Yang X, Liu J, Qiu S W, Cao M T, Chen H X, Wei D, Müller-Dethlefs K, Gao H and Li F L 2020 *J. Phys. Commun.* **4** 015019
[25] Li Y K, Wang J W, Yang X, Chen Y, Chen X Y, Cao M T, Wei D, Gao H and Li F L 2019 *Chin. Phys. B* **28** 014205